Adaptive Synchronization Control of Multiple Spacecraft Formation Flying

Hong-Tao Liu
The Institute for Aerospace Studies
University of Toronto
4925 Dufferin St., Toronto, Canada M3H 5T6

Jinjun Shan
Department of Earth and Space Science and Engineering
York University
4700 Keele St., Toronto, Canada M3J 1P3

Dong Sun
Department of Manufacturing Engineering and Engineering Management
City University of Hong Kong
83 Tat Chee Ave., Hong Kong

Abstract

An adaptive nonlinear synchronization control approach is developed for multiple spacecraft formation flying with elliptical reference orbits. It can guarantee that both the tracking errors and the synchronization errors of the relative positions converge to zero globally, even in the presence of uncertain parameters. The generalized synchronization concept allows to design various synchronization errors so that different synchronization performance can be obtained. Simulation results of a leader-follower spacecraft pair and the maneuvering of multiple spacecraft in formation flying are presented to verify the effectiveness of the proposed control technique.

1 Introduction

NASA and the U.S. Air force have identified Multiple Spacecraft Formation Flying (MSFF) as an enabling technology for future missions, which has led to a number of studies on MSFF, such as dynamics, control, and navigation. For control aspect, a lot of controllers have been designed and applied to MSFF, for example LQR [1], decentralized control [2], intelligent control [3], adaptive control [4, 5], coordination and synchronization control [6, 7].

In this paper, we apply the cross-coupling concept [8, 9] to the MSFF and propose an adaptive synchronization control strategy for MSFF. This controller can guarantee the convergences of both the relative position tracking errors and the position tracking synchronization errors, i.e. the relative position tracking errors converge to 0 at the same rate. This approach can be used in the case where maneuvers of multiple spacecraft in formation are needed to accelerate the maneuver process and reduce the response time. This control approach can also be applied to the synchronous attitude rotation of multiple spacecraft about single/multiple given axes, which is useful in the continuous observation of a planetary surface using cameras attached to a number of spacecraft [7].

2 Modeling of Spacecraft Formation Flying

The dynamics of spacecraft formation flying has been studied by many researchers. For the leader spacecraft runs in an elliptical orbit, the relative motion between the leader and the follower spacecraft is governed by the following nonlinear equation [4, 5]

$$m_f\ddot{\mathbf{q}} + \mathbf{C}(\omega)\dot{\mathbf{q}} + \mathbf{N}(\mathbf{q}, \omega, \dot{\omega}, R_l, \mathbf{u}_l) + \mathbf{F}_d = \mathbf{u}_f \tag{1}$$

where m_f is the mass of the follower spacecraft, the relative position vector $\mathbf{q} \in \mathbb{R}^3 \triangleq [x(t) \quad y(t) \quad z(t)]^T$, ω and $\dot{\omega}$ are the orbit angular velocity and acceleration, R_l is the distance from the Earth to the leader spacecraft, $\mathbf{u}_f \in \mathbb{R}^3 \triangleq [u_{fx} \quad u_{fy} \quad u_{fz}]^T$ and $\mathbf{u}_l \in \mathbb{R}^3 \triangleq [u_{lx} \quad u_{ly} \quad u_{lz}]^T$ are the control vectors for the follower and the leader spacecraft, $\mathbf{F}_d \in \mathbb{R}^3 \triangleq [F_{dx} \quad F_{dy} \quad F_{dz}]^T$ is the constant disturbance difference vector, the Coriolis-like matrix $\mathbf{C}(\omega) \in \mathbb{R}^{3\times3}$ and the nonlinear term $\mathbf{N}(\mathbf{q}, \omega, \dot{\omega}, R_l, \mathbf{u}_l) \in \mathbb{R}^3$ are

$$\mathbf{C}(\omega) = 2m_f\omega \begin{bmatrix} 0 & 1 & 0 \\ -1 & 0 & 0 \\ 0 & 0 & 0 \end{bmatrix} \quad \mathbf{N}(\cdot) = \begin{bmatrix} m_f\mu\mathcal{K}(x, y, z, R_l)x - m_f\omega^2 x + m_f\dot{\omega}y + \dfrac{m_f}{m_l}u_{lx} \\ m_f\mu\left[\mathcal{K}(x, y, z, R_l)(y + R_l) - R_l^{-2}\right] - m_f\omega^2 y - m_f\dot{\omega}x + \dfrac{m_f}{m_l}u_{ly} \\ m_f\mu\mathcal{K}(x, y, z, R_l)z + \dfrac{m_f}{m_l}u_{lz} \end{bmatrix} \tag{2}$$

with $\mathcal{K}(x, y, z, R_l) \triangleq \left[x^2 + (R_l + y)^2 + z^2\right]^{-\frac{3}{2}}$.

Following a similar procedure as that in [4], the following linear parameterized equation for Eq. (1) can be obtained

$$m_f\mathbf{p} + \mathbf{C}(\omega)\dot{\mathbf{q}} + \mathbf{N}(\mathbf{q}, \omega, \dot{\omega}, R_l, \mathbf{u}_l) + \mathbf{F}_d = \mathbf{W}(\mathbf{p}, \dot{\mathbf{q}}, \mathbf{q}, \omega, \dot{\omega}, R_l, \mathbf{u}_l)\boldsymbol{\Theta} = \mathbf{u}_f \tag{3}$$

where $\mathbf{p} \in \mathbb{R}^3 \triangleq [p_x \quad p_y \quad p_z]^T$ is a dummy variable, $\mathbf{W}(\cdot) \in \mathbb{R}^{3\times5}$ is the regressor matrix that is composed of known functions, $\boldsymbol{\Theta} \in \mathbb{R}^4 \triangleq [m_f \quad F_{dx} \quad F_{dy} \quad F_{dz}]^T$ is the system's constant parameter vector and $\widehat{\boldsymbol{\Theta}}(t)$ is defined as its estimate vector, and $\mathbf{W}(\cdot)$ can be explicitly defined as follows:

$$\mathbf{W}(\cdot) \triangleq \begin{bmatrix} p_x + 2\omega\dot{y} + \left[\mu\mathcal{K}(x, y, z, R_l) - \omega^2\right]x + \dot{\omega}y + \dfrac{1}{m_l}u_{lx} & 1 & 0 & 0 \\ p_y - 2\omega\dot{x} + \mu\left[\mathcal{K}(x, y, z, R_l)(y + R_l) - R_l^{-2}\right] - \dot{\omega}x - \omega^2 y + \dfrac{1}{m_l}u_{ly} & 0 & 1 & 0 \\ p_z + \mu\mathcal{K}(x, y, z, R_l)z + \dfrac{1}{m_l}u_{lz} & 0 & 0 & 1 \end{bmatrix} \tag{4}$$

3 Adaptive Synchronization Controller

The implementation of formation flying depends on accurate relative position control. In this paper, we first consider a leader-follower formation configuration to develop the controller. Then, we apply the controller to the case of multiple spacecraft formation flying.

By defining $\mathbf{q}_d(t) \in \mathbb{R}^3 = [x_d(t) \quad y_d(t) \quad z_d(t)]^T$ as the desired relative position trajectory and assuming its first two time derivatives are bounded, the position tracking error $\mathbf{e}(t) \in \mathbb{R}^3$ becomes

$$\mathbf{e}(t) \triangleq \mathbf{q}_d(t) - \mathbf{q}(t) \tag{5}$$

3.1 Generalized Synchronization Error

Synchronization error is used to identify the performance of the synchronization controller, i.e. how one trajectory converges with respect to each other. There are various ways to choose the synchronization error. In this paper, we propose the following synchronization error $\mathbf{\Xi}(t)$, which is a linear combination of position tracking error $\mathbf{e}(t)$

$$\mathbf{\Xi}(t) = \mathbf{T}\mathbf{e}(t) \tag{6}$$

where $\mathbf{\Xi} \triangleq [\varepsilon_1 \quad \varepsilon_2 \quad \cdots \quad \varepsilon_n]^T \in \mathbb{R}^{n\times 1}$, $\mathbf{T} \in \mathbb{R}^{n\times n}$ is a generalized synchronization transformation matrix.

By choosing different matrix $\mathbf{T}$, we can form different synchronization errors. In our investigation, we choose the following synchronization transformation matrix

$$\mathbf{T} = \begin{bmatrix} 2 & -1 & & & -1 \\ -1 & 2 & -1 & & \\ & \ddots & \ddots & \ddots & \\ & & -1 & 2 & -1 \\ -1 & & & -1 & 2 \end{bmatrix} \tag{7}$$

From Eqs. (6, 7) we know that, if $\mathbf{e}(t) \to 0$ and $\mathbf{\Xi}(t) \to 0$ can be realized at the same time, $e_i(t)$ $(i = 1,\ 2,\ 3)$ will go to zero at the same rate. Therefore the control objective becomes to achieve $\mathbf{e}(t) \to 0$ and $\mathbf{\Xi}(t) \to 0$ as $t \to \infty$ in the presence of unknown parameters.

3.2 Controller Development

For controller design, a coupled position error $\mathbf{e}^*(t) \triangleq [e_1^* \quad e_2^* \quad \cdots \quad e_n^*]^T \in \mathbb{R}^n$, which contains both the position tracking error $\mathbf{e}(t)$ and the synchronization error $\mathbf{\Xi}(t)$, is further introduced [9]

$$\mathbf{e}^*(t) = \mathbf{e}(t) + \mathbf{B}\mathbf{T}^T \int_0^t \mathbf{\Xi} d\tau \tag{8}$$

where $\mathbf{B} \triangleq \mathrm{diag}[\beta \quad \beta \quad \cdots \quad \beta]$ is a positive coupling gain matrix, the corresponding coupled velocity error is $\dot{\mathbf{e}}^*(t) = \dot{\mathbf{e}}(t) + \mathbf{B}\mathbf{T}^T\mathbf{\Xi}(t)$, and the detailed coupled position error is

$$\begin{aligned}
e_1^*(t) &= e_1(t) + \beta \int_0^t (2\varepsilon_1(\tau) - \varepsilon_2(\tau) - \varepsilon_n(\tau))d\tau \\
e_2^*(t) &= e_2(t) + \beta \int_0^t (2\varepsilon_2(\tau) - \varepsilon_3(\tau) - \varepsilon_1(\tau))d\tau \\
&\vdots \\
e_n^*(t) &= e_n(t) + \beta \int_0^t (2\varepsilon_n(\tau) - \varepsilon_{n-1}(\tau) - \varepsilon_1(\tau))d\tau
\end{aligned} \tag{9}$$

It can be seen from Eq. (9) that the synchronization error $\varepsilon_i(t)$ appears in $e_i^*(t)$ as $2\varepsilon_i(t)$ and $-\varepsilon_i(t)$ in $e_{i+1}^*(t)$ and $e_{i+1}^*(t)$. In this way, the coupled position errors are driven in opposite directions by $\varepsilon_i(t)$, which contributes to the elimination of the synchronization error $\varepsilon_i(t)$.

The coupled filtered tracking error, $\mathbf{r}(t) \in \mathbb{R}^n$, is defined as [4, 9]

$$\mathbf{r}(t) = \dot{\mathbf{e}}^*(t) + \mathbf{\Lambda}\mathbf{e}^*(t) \tag{10}$$

with the constant, diagonal, positive-definite, control gain matrix $\mathbf{\Lambda} \in \mathbb{R}^{n\times n}$.

Then the controller is designed to contain an adaptation on-line estimation law for unknown parameter $\mathbf{\Theta}$ and feedback terms

$$\mathbf{u}_f(t) = \mathbf{W}(\cdot)\widehat{\mathbf{\Theta}}(t) + \mathbf{K}\mathbf{r}(t) + \mathbf{K}_s\mathbf{T}^T\mathbf{\Xi}(t) \tag{11}$$

where $\mathbf{K} \in \mathbb{R}^{n\times n}$, $\mathbf{K}_s \in \mathbb{R}^{n\times n}$ are two constant, diagonal, positive-definite control gain matrices, and the estimated parameter $\widehat{\mathbf{\Theta}}(t)$ is subject to the following adaptation law

$$\dot{\widehat{\mathbf{\Theta}}} = \mathbf{\Gamma}\mathbf{W}^T(\cdot)\mathbf{r} \tag{12}$$

with the constant, diagonal, positive-definite, adaptation gain matrix $\mathbf{\Gamma} \in \mathbb{R}^{4\times 4}$.

Therefore, the closed-loop dynamics for the parameter estimation error vector $\widetilde{\mathbf{\Theta}}(t) \triangleq \mathbf{\Theta} - \widehat{\mathbf{\Theta}}(t)$ is

$$\dot{\widetilde{\mathbf{\Theta}}} = -\mathbf{\Gamma}\mathbf{W}^T(\cdot)\mathbf{r} \tag{13}$$

Moreover, the dummy variable $\mathbf{p}$ in Eq. (3) has the following expression

$$\mathbf{p} = \ddot{\mathbf{q}}_d + \mathbf{\Lambda}\dot{\mathbf{e}}^* + \mathbf{B}\mathbf{T}^T\dot{\mathbf{\Xi}} \tag{14}$$

Theorem 1. The proposed adaptive synchronization controller Eqs. (10, 11, 12) guarantees the global asymptotic convergences to zero of both the position tracking error $\mathbf{e}(t)$ and the position synchronization error $\mathbf{\Xi}(t)$, i.e.

$$\lim_{t\to\infty} \mathbf{e}(t),\ \mathbf{\Xi}(t) = 0 \tag{15}$$

Proof. Define the following positive definite Lyapunov function

$$V(\mathbf{r}, \widetilde{\mathbf{\Theta}}, \mathbf{\Xi}) \triangleq \frac{1}{2}\mathbf{r}^T m_f \mathbf{r} + \frac{1}{2}\widetilde{\mathbf{\Theta}}^T \mathbf{\Gamma}^{-1}\widetilde{\mathbf{\Theta}} + \frac{1}{2}\mathbf{\Xi}^T \mathbf{K}_s \mathbf{\Xi} + \frac{1}{2}\Big(\int_0^t \mathbf{T}^T \mathbf{\Xi} \mathrm{d}\tau\Big)^T \mathbf{B}\mathbf{\Lambda}\mathbf{K}_s \Big(\int_0^t \mathbf{T}^T \mathbf{\Xi} \mathrm{d}\tau\Big) \tag{16}$$

and its derivative with respect to time t is

$$\dot{V}(\mathbf{r}, \widetilde{\mathbf{\Theta}}, \mathbf{\Xi}) = \mathbf{r}^T m_f \dot{\mathbf{r}} + \widetilde{\mathbf{\Theta}}^T \mathbf{\Gamma}^{-1}\dot{\widetilde{\mathbf{\Theta}}} + \mathbf{\Xi}^T \mathbf{K}_s \dot{\mathbf{\Xi}} + \Big(\int_0^t \mathbf{T}^T \mathbf{\Xi} \mathrm{d}\tau\Big)^T \mathbf{B}\mathbf{\Lambda}\mathbf{K}_s \mathbf{T}^T \mathbf{\Xi} \tag{17}$$

After some mathematical manipulations, we can get

$$\dot{V}(\mathbf{r}, \widetilde{\mathbf{\Theta}}, \mathbf{\Xi}) = -\mathbf{r}^T \mathbf{K}\mathbf{r} - (\mathbf{T}^T\mathbf{\Xi})^T \mathbf{B}\mathbf{K}_s(\mathbf{T}^T\mathbf{\Xi}) - \mathbf{\Xi}^T \mathbf{\Lambda}\mathbf{K}_s \mathbf{\Xi} \leq 0 \tag{18}$$

Following the standard process as that in [10], all signals in the adaptive synchronization controller and system can be proved to be bounded during the closed-loop operation.

From Eq. (18), we have $\mathbf{r}(t) \in \mathcal{L}_2$, $\mathbf{T}^T\mathbf{\Xi}(t) \in \mathcal{L}_2$ and $\mathbf{\Xi}(t) \in \mathcal{L}_2$. Hence, $\lim_{t\to\infty} \mathbf{r}(t) = 0$ and $\lim_{t\to\infty} \mathbf{\Xi}(t) = 0$ can be obtained according to Corollary 1.1 in [10]. Furthermore, we can conclude that $\lim_{t\to\infty} \mathbf{e}^*(t), \dot{\mathbf{e}}^*(t) = 0$ using Lemma 1.6 in [10]. When $\mathbf{\Xi}(t) = 0$, one can get $e_1(t) = e_2(t) = \cdots = e_n(t) = 0$ by considering $\lim_{t\to\infty} \mathbf{e}^*(t) = 0$ and the form of the synchronization matrix in Eq. (7). Also from Eq. (18), we know that $\dot{V}(\cdot) = 0$ only if $\mathbf{e}(t) = 0$. Therefore, $\lim_{t\to\infty} \mathbf{e}(t) = 0$ can be concluded using LaSalle's theorem [11]. Thus we finally reach

$$\lim_{t\to\infty} \mathbf{e}(t),\ \mathbf{\Xi}(t) = 0$$

4 Simulation Results

4.1 Leader-Follower Spacecraft Pair

A leader-follower formation flying configuration is considered in this section. The leader spacecraft runs in an elliptical orbit with orbital elements: semi-major axis $a = 42241$ km, eccentricity $e = 0.2$ and mean motion $n = 7.2722 \times 10^{-5}$ rad/s. The masses of the leader and the follower spacecraft are $m_l = 1550$ kg and $m_f = 410$ kg. $\mathbf{F}_d = [-1.025 \quad 6.248 \quad -2.415]^T \times 10^{-5}$ N. The desired relative position trajectory is chosen to be $x_d(t) = 100\sin(4\omega t)[1.0 - \exp(-0.05t^3)]$ m, $y_d(t) = 100\cos(4\omega t)[1.0 - \exp(-0.05t^3)]$ m, $z_d(t) = 0$ m, and the initial conditions are $\mathbf{q}(0) = [30 \quad 0 \quad -200]^T$ m, $\dot{\mathbf{q}}(0) = [0 \quad 0 \quad 0]^T$ m/s, $\widehat{\mathbf{\Theta}}(0) = \mathrm{diag}[0.8 \quad 0.7 \quad 0.7 \quad 0.8]\mathbf{\Theta}$. The control and adaptation gains are $\mathbf{K} = \mathrm{diag}[0.13 \quad 0.12 \quad 0.09]$, $\mathbf{K}_s = \mathrm{diag}[0.03 \quad 0.03 \quad 0.03]$, $\mathbf{\Lambda} = \mathrm{diag}[0.04 \quad 0.04 \quad 0.04]$, $\mathbf{\Gamma} = \mathrm{diag}[900 \quad 28 \quad 28 \quad 9] \times 10^{-5}$, and $\mathbf{B} = \mathrm{diag}[8.0 \quad 8.0 \quad 8.0] \times 10^{-4}$.

Figure 1 shows the simulation results of adaptive tracking control of formation flying without synchronization strategy. Figure 2 gives the corresponding simulation results with synchronization strategy. For the purpose of comparison, the 2-norms of $\mathbf{e}(t)$ and $\boldsymbol{\Xi}(t)$ after 5 hours are calculated for all simulations and listed in Table 1. It can be seen from the results that although the position tracking error vector $\mathbf{e}(t) \to 0$ can be achieved by using the adaptive controller without synchronization strategy, the differences between the position tracking errors of all axes are large, i.e. the synchronization errors are large. However, with the proposed adaptive synchronization controller, the synchronization performance can be observably improved. Take X-axis as an example, the 2-norms of the position tracking error and the synchronization error are 341.5 m and 1442.8 m, respectively, without synchronization strategy. With synchronization strategy, the corresponding 2-norms have become 940.8 m and 150.7 m. The synchronization error has been remarkably reduced. Moreover, Table 1 shows the control efforts needed for performing these control strategies. The results show that more fuel consumption is needed for using synchronization controller. For example, to maneuver and maintain the X-axis relative position in 30 hours with the adaptive controller, a fuel consumption of 382.1 N·s is needed. However, 742.6 N·s is necessary for using the synchronization strategy.

4.2 Multiple Spacecraft in Formation

In this section, we assume four spacecraft are requested to maneuver from their initial relative positions $\mathbf{R}_{i0}$ ($i = 1,\ 2,\ 3,\ 4$) to the final positions $\mathbf{R}_{if}$ along the following trajectory and to form a circular formation

$$\mathbf{R}_i^d(t) = \mathbf{R}_{i0} + (\mathbf{R}_{if} - \mathbf{R}_{i0}) \cdot \left[1 - \exp(C_i t^3)\right] \tag{19}$$

where $C_1 = -0.01$, $C_2 = -0.02$, $C_3 = -0.03$, $C_4 = -0.04$.

For this case, we can apply the synchronization strategy in two ways: internal and external. The internal synchronization error, $\boldsymbol{\Xi}(t)$, is the synchronization error between different axes of one spacecraft. This is the same as that in the leader-follower configuration. The external synchronization error $\mathbf{E}(t)$, however, denotes the synchronization error between a given axis of all spacecraft. Therefore, the total coupled position error becomes

$$\mathbf{e}^*(t) = \mathbf{e}(t) + \mathbf{B}'\mathbf{T}_\beta \int_0^t \boldsymbol{\Xi}(\tau)d\tau + \mathbf{A}'\mathbf{T}_E\mathbf{T}_\alpha \int_0^t \mathbf{E}(\tau)d\tau \tag{20}$$

where m denotes the spacecraft number, n is the number of axes of one spacecraft, $\mathbf{e} = [\mathbf{e}_1^T \quad \mathbf{e}_2^T \quad \cdots \quad \mathbf{e}_m^T]^T$, $\mathbf{e}^* = [\mathbf{e}_1^{*T} \quad \mathbf{e}_2^{*T} \quad \cdots \quad \mathbf{e}_m^{*\,T}]^T$, $\boldsymbol{\Xi} = [\boldsymbol{\Xi}_1^T \quad \boldsymbol{\Xi}_2^T \quad \cdots \quad \boldsymbol{\Xi}_m^T]^T$, $\mathbf{E} = [\mathbf{E}_1^T \quad \mathbf{E}_2^T \quad \cdots \quad \mathbf{E}_n^T]^T \in \mathbb{R}^{mn\times 1}$, $\mathbf{e}_i = [e_{i1} \quad e_{i2} \quad \cdots \quad e_{in}]^T$, $\mathbf{e}_i{}^* = [e_{i1}{}^* \quad e_{i2}{}^* \quad \cdots \quad e_{in}{}^*]^T$, $\boldsymbol{\Xi}_i = [\varepsilon_{i1} \quad \varepsilon_{i2} \quad \cdots \quad \varepsilon_{in}]^T \in \mathbb{R}^{n\times 1}$, $\mathbf{E}_i = [\epsilon_{1i} \quad \epsilon_{2i} \quad \cdots \quad \epsilon_{mi}]^T \in \mathbb{R}^{m\times 1}$, $\mathbf{B}' = \mathrm{diag}[\mathbf{B}_1^T \quad \mathbf{B}_2^T \quad \cdots \quad \mathbf{B}_m^T]$, $\mathbf{A}' = \mathrm{diag}[\mathbf{A}_1^T \quad \mathbf{A}_2^T \quad \cdots \quad \mathbf{A}_m^T] \in \mathbb{R}^{mn\times mn}$ are two diagonal synchronization gain matrices, $\mathbf{B}_i = [\beta_{i1} \quad \beta_{i2} \quad \cdots \quad \beta_{in}]^T$, $\mathbf{A}_i = [\alpha_{i1} \quad \alpha_{i2} \quad \cdots \quad \alpha_{in}]^T$, $\mathbf{T}_\beta = \mathrm{diag}[\mathbf{T}_{\beta 1} \quad \mathbf{T}_{\beta 2} \quad \cdots \quad \mathbf{T}_{\beta m}] \in \mathbb{R}^{mn\times mn}$ is the internal synchronization transformation matrix with $\mathbf{T}_{\beta i} \in \mathbb{R}^{n\times n}$, $\mathbf{T}_\alpha = \mathrm{diag}[\mathbf{T}_{\alpha 1} \quad \mathbf{T}_{\alpha 2} \quad \cdots \quad \mathbf{T}_{\alpha n}] \in \mathbb{R}^{mn\times mn}$

is the external synchronization transformation matrix with $\mathbf{T}_{\alpha i} \in \mathbb{R}^{m \times m}$, and another transformation matrix $\mathbf{T}_E$ is

$$\mathbf{T}_E = \begin{cases} 1 & \text{for} \quad ((i-1)n+j, (j-1)m+i); \quad i = 1, 2, \cdots, m \\ 0 & \text{for} \quad \text{others}; \qquad\qquad\qquad\qquad\quad j = 1, 2, \cdots, n \end{cases}$$

Figure 3 gives the simulation results using internal synchronization strategy only. Figure 4 gives the results with both internal and external synchronization strategies. Table 2 shows the parameters and control gains for MSFF simulation. Other gains are kept the same as those in the leader-follower configuration. It can be seen from these simulation results that the synchronization errors of these four spacecraft about any given axis, X, Y and Z, have been remarkably reduced by applying the external synchronization strategy.

5 Conclusions

This paper presents the development of an adaptive nonlinear synchronization controller for Multiple Spacecraft Formation Flying (MSFF). With this controller, both the position tracking errors and the position synchronization errors can be guaranteed to globally converge to zero even in the presence of uncertain parameters. Different from the previous adaptive controllers for formation flying, this controller can achieve synchronized motion among multiple axes of one spacecraft and/or any given axis of multiple spacecraft while realizing the convergences of position tracking errors. Simulations are conducted on the leader-follower configuration and multiple spacecraft formation flying to verify the effectiveness of the proposed controller. Future work under consideration includes: 1) adaptive synchronization control for MSFF with time-varying parameters; 2) adaptive synchronization control for MSFF with synchronization between translational (orbital) motion and attitude motion.

References

[1] Vassar, R. H., and Sherwood, R. B., 1985. "Formationkeeping for a pair of satellites in a circular orbit". Journal of Guidance, Control and Dynamics, **8**(2), pp. 235–242.

[2] Carpenter, J. R., 2002. "Decentralized control of satellite formations". International Journal of Robust and Nonlinear Control, **12**(2-3), pp. 141–161.

[3] Vadali, S. R., Vaddi, S. S., and Alfriend, K. T., 2002. "An intelligent control concept for formation flying satellites". International Journal of Robust and Nonlinear Control, **12**(2-3), pp. 97–115.

[4] de Queiroz, M. S., Kapila, V., and Yan, Q., 2000. "Adaptive nonlinear control of multiple spacecraft formation flying". Journal of Guidance, Control and Dynamics, **23**(3), pp. 385–390.

[5] Wong, H., and Kapila, V., 2003. "Adaptive learning control-based periodic trajectory tracking for spacecraft formations". In Proceedings of the 42nd IEEE Conference on Decision and Control, pp. 3597–3602.

[6] Kang, W., Sparks, A., and Banda, S., 2001. "Coordinated control of multisatellite systems". Journal of Guidance, Control and Dynamics, **24**(2), pp. 360–368.

[7] Wang, P. K. C., Hadaegh, F. Y., and Lau, K., 1999. "Synchronized formation rotation and attitude control of multiple free-flying spacecraft". Journal of Guidance, Control and Dynamics, **22**(1), pp. 28–35.

[8] Koren, Y., 1980. "Cross-coupled biaxial computer controls for manufacturing systems". ASME Journal of Dynamic Systems, Measurement, and Control, **102**(2), pp. 256–272.

[9] Sun, D., 2003. "Position synchronization of multiple motion axes with adaptive coupling control". Automatica, **39**(6), pp. 997–1005.

[10] Dawson, D. M., Hu, J., and Burg, T. C., 1998. *Nonlinear Control of Electric Machinery.* Marcel Dekker, Inc.

[11] Khalil, H., 1996. *Nonlinear Systems*, 2nd ed. Prentice Hall.

Table 1 Performance evaluation wihtout/with synchronization strategy

Error/Control	Without	With
$\|\|e_x\|\|_2$ (m)	78.8	940.8
$\|\|e_y\|\|_2$ (m)	341.5	940.8
$\|\|e_z\|\|_2$ (m)	1540.1	887.3
$\|\|\varepsilon_x\|\|_2$ (m)	419.2	88.1
$\|\|\varepsilon_y\|\|_2$ (m)	1442.8	150.7
$\|\|\varepsilon_z\|\|_2$ (m)	1576.7	160.3
$\int \|u_{xf}\|$ $(N{\cdot}s)$	382.1	742.6
$\int \|u_{yf}\|$ $(N{\cdot}s)$	498.9	527.9
$\int \|u_{zf}\|$ $(N{\cdot}s)$	115.7	424.0

Table 2 Parameters of multiple spacecraft in formation flying

Parameter	Value ($i = 1,\ 2,\ 3,\ 4$)
m_{fi} (kg)	410, 500, 600, 660
$\mathbf{F}_{di}(\times 10^{-5})$ (N)	[-1.025, 6.248, -2.415], [1.9106, -1.960, -1.517]
	[-1.925, 4.850, -2.455], [-2.250, 6.850, -3.156]
$\mathbf{R}_{i0}$ (m)	[150, 10, 20], [-10, -130, -20]
	[-140, 10, -20], [30, 160, 20]
$\dot{\mathbf{R}}_{i0}$ (m)	[0, 0, 0]
$\mathbf{R}_{if}$ (m)	[100, 0, 0], [0, -100, 0], [-100, 0, 0], [0, 100, 0]
$\dot{\mathbf{R}}_{if}$ (m)	[0, 0, 0]
$\widehat{\mathbf{\Theta}}(0)$	0.7$\mathbf{\Theta}$, 0.85$\mathbf{\Theta}$, 1.15$\mathbf{\Theta}$, 1.3$\mathbf{\Theta}$
$\mathbf{B}_i$ $(\times 10^{-3})$	[8.0, 8.0, 8.0]
$\mathbf{A}_i$ $(\times 10^{-3})$	[8.0, 8.0, 8.0]

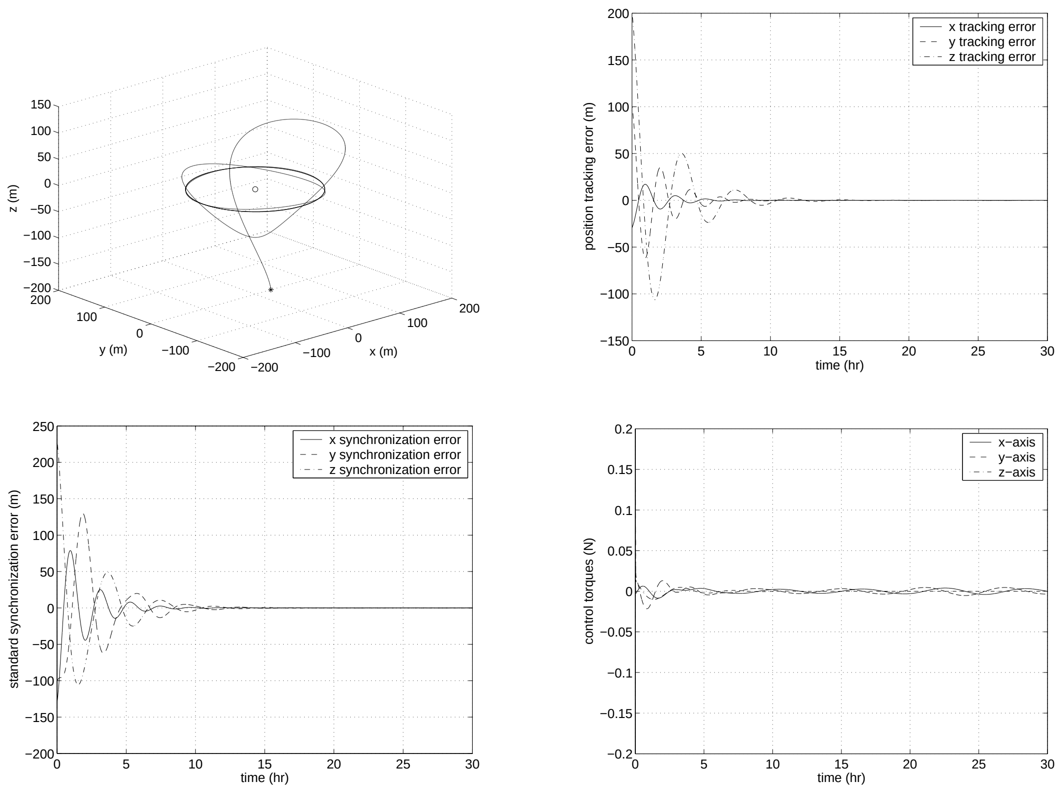

Fig. 1 Simulation results of adaptive tracking control of formation flying without synchronization strategy

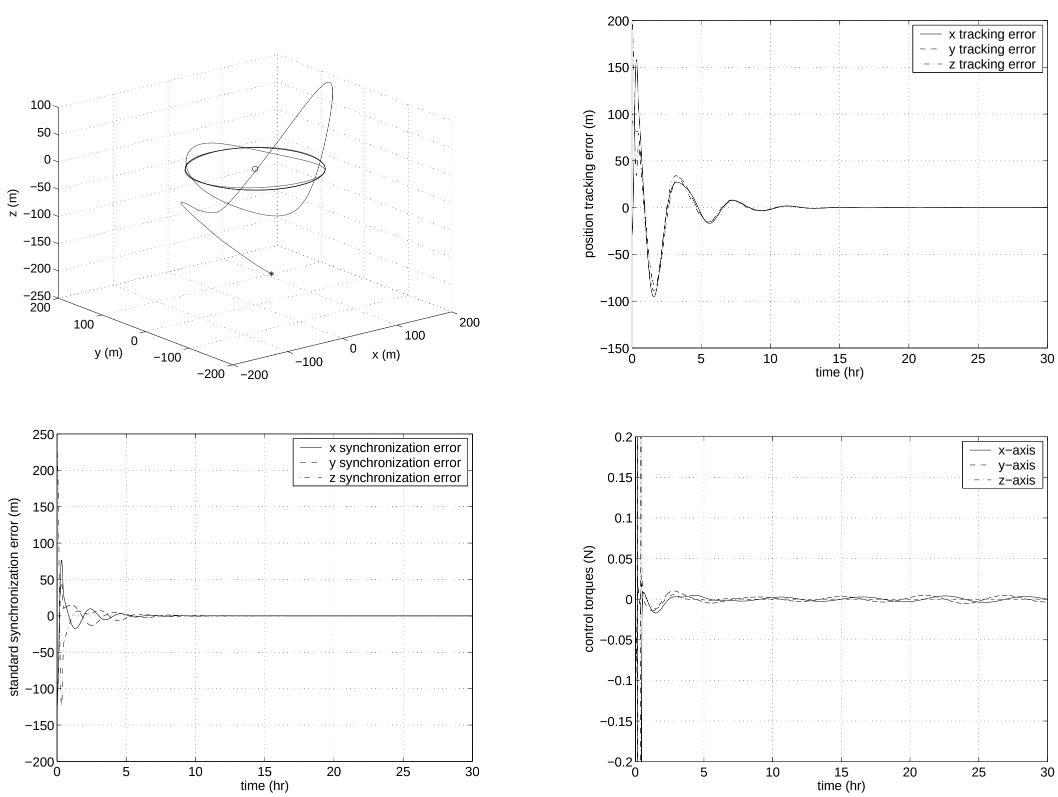

Fig. 2 Simulation results of adaptive tracking control of formation flying with synchronization strategy

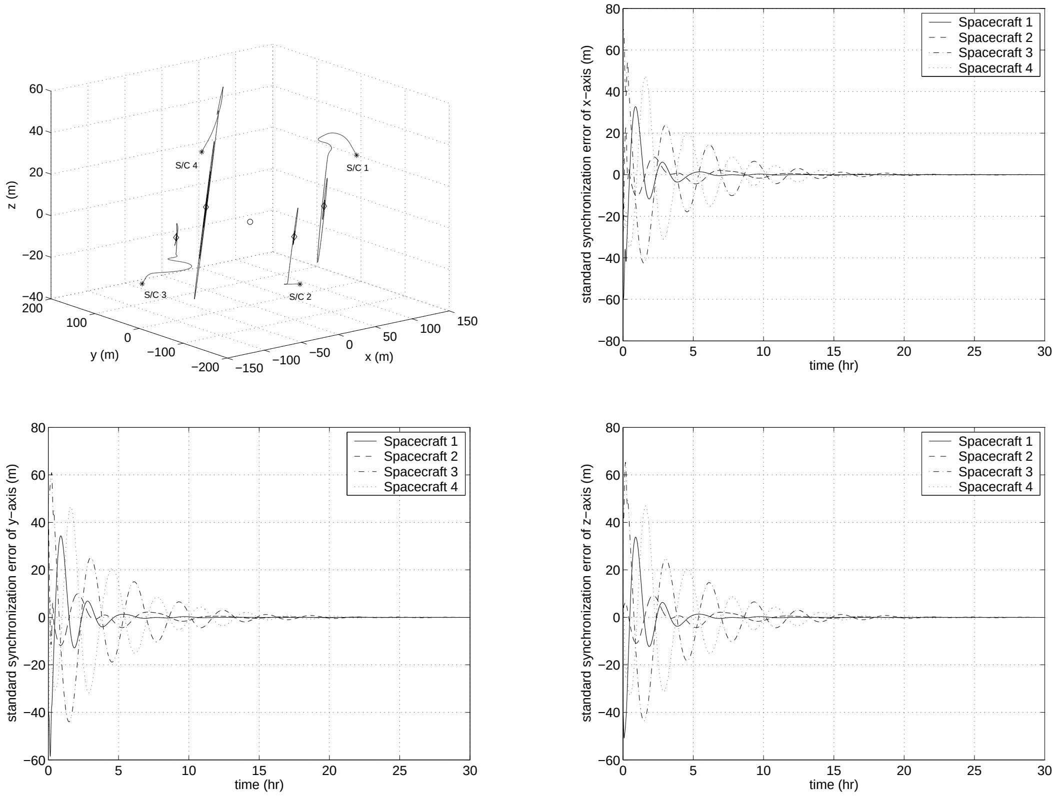

Fig. 3 Simulation results of adaptive control of multiple spacecraft in formation flying with only internal synchronization strategy

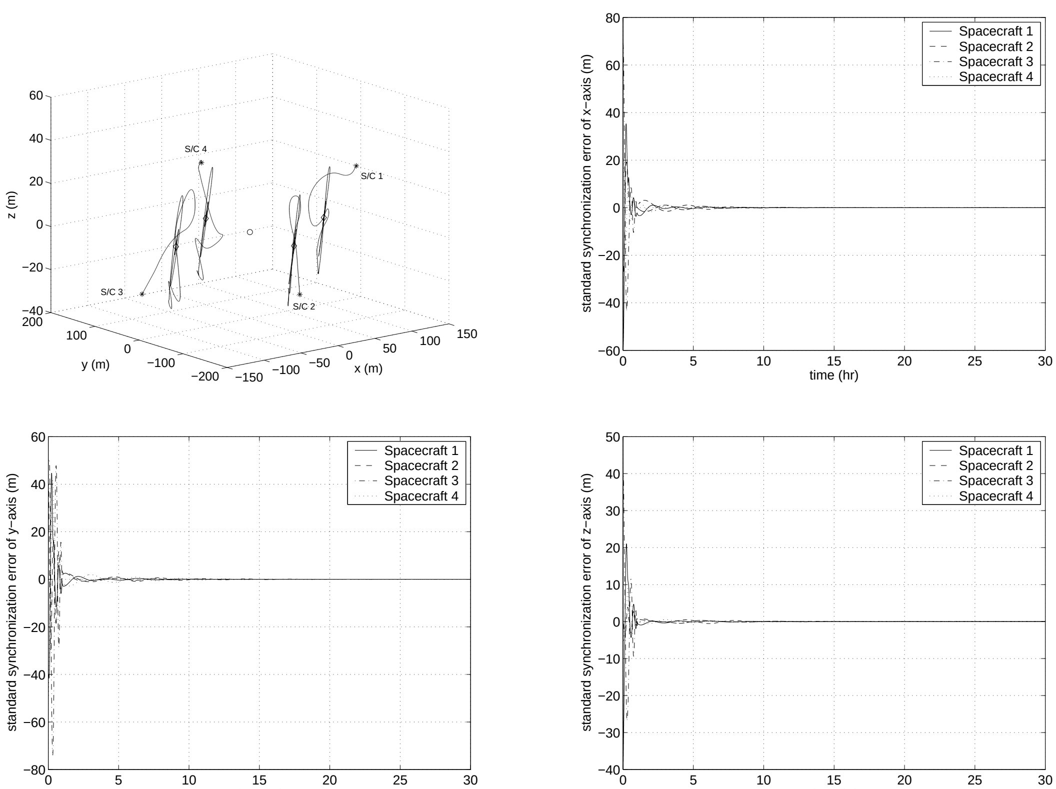

Fig. 4 Simulation results of adaptive control of multiple spacecraft in formation flying with both internal and external synchronization strategy